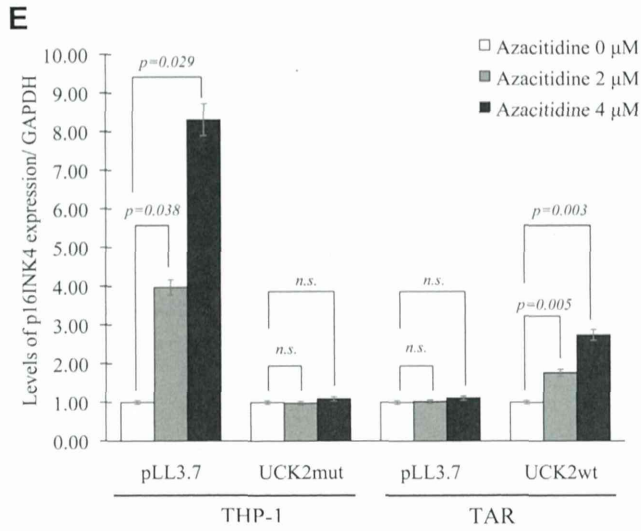


**Figure 5.** (*continued*). **(E)** Cells transfected with PLL3.7 or each *UCK2* expression vector were cultured in the absence or presence of indicated concentrations of azacitidine for 24 hours. Total RNA was prepared from the cells, and the levels of *p16* mRNA were determined with real-time PCR analyses. *GAPDH* cDNA was used as an internal control. The results were calculated using the $DDC_T$ method and are expressed as the ratio of *p16* mRNA level in cells treated with azacitidine to that in untreated cells. Statistical analysis was performed using Student *t* test for comparison of the data between untreated cells and cells treated with azacitidine. UCK2mut = expression vector of mutated *UCK2*; UCK2wt = expression vector of wild type *UCK2*.

cell line that was resistant to potent inhibitors of RNA polymerases 3′-ethynyl nucleosides [36]. They also found a point mutation in exon 4 of *UCK2* in the 3′-ethynyl nucleosides-resistant human gastric carcinoma cell line [36]. Therefore, it is highly possible that diminishment of UCK2 activity is critical for acquisition of resistance to other anticancer drugs as well. In the previously reported decitabine-resistant cells, the level of DCK decreased because of a *DCK* gene mutation, resulting in the acquisition of resistance to decitabine as well as cytarabine, a key drug for leukemia treatment [23,37]. In TAR and HAR cells, however, the level of UCK2 protein did not decrease, suggesting that those mutations diminish UCK activity without affecting the expression level of this enzyme.

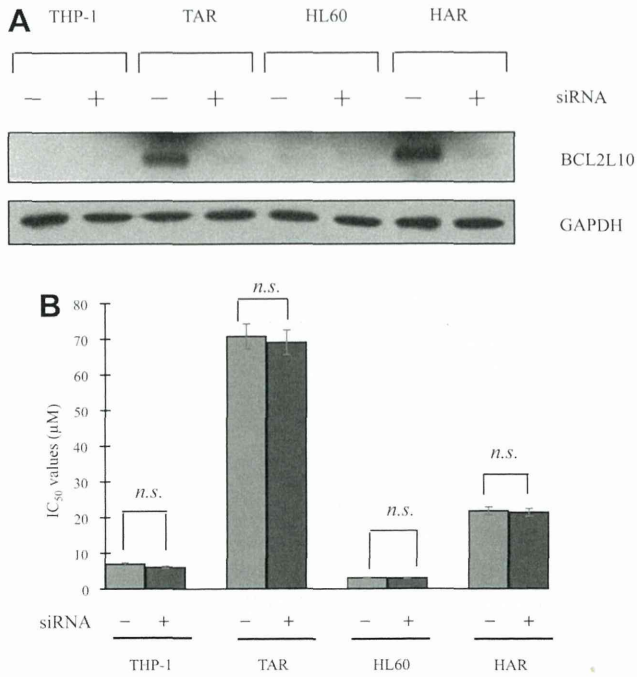


**Figure 6.** siRNA-mediated knockdown of BCL2L10 resulted in no restoration of azacitidine sensitivity in TAR and HAR cells. **(A)** Cells were transfected with BCL2L10 siRNA as described in Methods. Total cell lysates were prepared from the cells and subjected to Western blot analysis using antibody against human BCL2L10. The expression of GAPDH is shown as an internal control. **(B)** Cells were transfected with BCL2L10 siRNA and cultured for 24 hours before treatment with azacitidine. After the addition of azacitidine, further incubation was performed for 96 hours and $IC_{50}$ values of azacitidine were determined.

Cluzeau T et al. showed that high expression of BCL2L10 was linked to drug resistance in their azacitidine-resistant cell line SKM1-R [24]. The azacitidine activation process might have been intact in SKM1-R cells, because they showed that siRNA-mediated suppression of BCL2L10 restored azacitidine sensitivity. In our study, we found that the protein level of BCL2L10 increased in both TAR and HAR cells (Fig. 6A). However, in our resistant cells, siRNA-mediated knockdown of BCL2L10 resulted in no restoration of sensitivity to azacitidine (Fig. 6B). These phenomena are consistent with our conclusion that azacitidine could not be activated because of *UCK2* gene mutations, regardless of the level of BCL2L10.

It is of great importance to clarify whether *UCK2* gene mutations are present in primary cells from azacitidine-resistant patients and are central to the resistance mechanism. Although we have not yet analyzed sufficient numbers of patients, such research is now proceeding in our laboratory. It is also of interest to clarify whether other resistance mechanisms are also observed in primary cells.

Our newly established azacitidine-resistant cell lines THP-1/AR and HL60/AR are opportune models to analyze the mechanisms of azacitidine resistance. Using these cell lines, we revealed that acquisition of resistance is primarily caused by a DNMT-dependent mechanism due to *UCK2* gene mutations. These cell lines might also be useful to search for agents, which could overcome resistance to azacitidine.

## Acknowledgments

We thank Gary Baley for academic editing, A. Izawa for technical assistance, and E. Yamakawa for preparation of the manuscript. This work was supported in part by grants-in-aid from the Ministry of Education, Culture, Sports, Science and Technology, Japan (25461435) and the Japan Leukemia Research Fund (to T.N.).

## Conflict of interest disclosure

No financial interest/relationships with financial interest relating to the topic of this article have been declared.

## References

1. Bird A. DNA methylation patterns and epigenetic memory. Genes Dev. 2002;16:6–21.
2. Jones PA, Baylin SB. The fundamental role of epigenetic events in cancer. Nat Rev Genet. 2002;3:415–428.
3. Christiansen DH, Andersen MK, Pedersen-Bjergaard J. Methylation of p15INK4B is common, is associated with deletion of genes on chromosome arm 7q and predicts a poor prognosis in therapy-related myelodysplasia and acute myeloid leukemia. Leukemia. 2003;17:1813–1819.
4. Herman JG, Baylin SB. Gene silencing in cancer in association with promoter hypermethylation. N Engl J Med. 2003;349:2042–2054.
5. Baylin SB. DNA methylation and gene silencing in cancer. Nat Clin Pract Oncol. 2005;2(Suppl 1):S4–S11.
6. Figueroa ME, Skrabanek L, Li Y, et al. MDS and secondary AML display unique patterns and abundance of aberrant DNA methylation. Blood. 2009;114:3448–3458.
7. Christman JK. 5-Azacytidine and 5-aza-2'-deoxycytidine as inhibitors of DNA methylation: mechanistic studies and their implications for cancer therapy. Oncogene. 2002;21:5483–5495.
8. Kuykendall JR. 5-azacytidine and decitabine monotherapies of myelodysplastic disorders. Ann Pharmacother. 2005;39:1700–1709.
9. Lubbert M. DNA methylation inhibitors in the treatment of leukemias, myelodysplastic syndromes and hemoglobinopathies: clinical results and possible mechanisms of action. Curr Top Microbiol Immunol. 2000;249:135–164.
10. Lubbert M, Wijermans P, Kunzmann R, et al. Cytogenetic responses in high-risk myelodysplastic syndrome following low-dose treatment with the DNA methylation inhibitor 5-aza-2'-deoxycytidine. Br J Haematol. 2001;114:349–357.
11. Sudan N, Rossetti JM, Shadduck RK, et al. Treatment of acute myelogenous leukemia with outpatient azacitidine. Cancer. 2006;107:1839–1843.
12. Keating GM. Azacitidine: a review of its use in higher-risk myelodysplastic syndromes/acute myeloid leukaemia. Drugs. 2009;69:2501–2518.
13. Ravandi F, Issa JP, Garcia-Manero G, et al. Superior outcome with hypomethylating therapy in patients with acute myeloid leukemia and high-risk myelodysplastic syndrome and chromosome 5 and 7 abnormalities. Cancer. 2009;115:5746–5751.
14. Fenaux P, Mufti GJ, Hellstrom-Lindberg E, et al. Efficacy of azacitidine compared with that of conventional care regimens in the treatment of higher-risk myelodysplastic syndromes: a randomised, open-label, phase III study. Lancet Oncol. 2009;10:223–232.
15. Santos FP, Kantarjian H, Garcia-Manero G, Issa JP, Ravandi F. Decitabine in the treatment of myelodysplastic syndromes. Expert Rev Anticancer Ther. 2010;10:9–22.
16. van der Helm LH, Veeger NJ, Kooy MV, et al. Azacitidine results in comparable outcome in newly diagnosed AML patients with more or less than 30% bone marrow blasts. Leuk Res. 2013;37:877–882.
17. Prebet T, Gore SD, Esterni B, et al. Outcome of high-risk myelodysplastic syndrome after azacitidine treatment failure. J Clin Oncol. 2011;29:3322–3327.
18. Damaraju VL, Damaraju S, Young JD, et al. Nucleoside anticancer drugs: the role of nucleoside transporters in resistance to cancer chemotherapy. Oncogene. 2003;22:7524–7536.
19. Kong W, Engel K, Wang J. Mammalian nucleoside transporters. Curr Drug Metab. 2004;5:63–84.
20. Pastor-Anglada M, Molina-Arcas M, Casado FJ, et al. Nucleoside transporters in chronic lymphocytic leukaemia. Leukemia. 2004;18:385–393.
21. Rius M, Stresemann C, Keller D, et al. Human concentrative nucleoside transporter 1-mediated uptake of 5-azacytidine enhances DNA demethylation. Mol Cancer Ther. 2009;8:225–231.
22. Kroep JR, Loves WJ, van der Wilt CL, et al. Pretreatment deoxycytidine kinase levels predict in vivo gemcitabine sensitivity. Mol Cancer Ther. 2002;1:371–376.
23. Qin T, Jelinek J, Si J, Shu J, Issa JP. Mechanisms of resistance to 5-aza-2'-deoxycytidine in human cancer cell lines. Blood. 2009;113:659–667.
24. Cluzeau T, Robert G, Mounier N, et al. BCL2L10 is a predictive factor for resistance to azacitidine in MDS and AML patients. Oncotarget. 2012;3:490–501.
25. Mahfouz RZ, Jankowska A, Ebrahem Q, et al. Increased CDA expression/activity in males contributes to decreased cytidine analog half-life and likely contributes to worse outcomes with 5-azacytidine or decitabine therapy. Clin Cancer Res. 2013;19:938–948.
26. Collins SJ, Gallo RC, Gallagher RE. Continuous growth and differentiation of human myeloid leukaemic cells in suspension culture. Nature. 1977;270:347–349.
27. Tsuchiya S, Yamabe M, Yamaguchi Y, et al. Establishment and characterization of a human acute monocytic leukemia cell line (THP-1). Int J Cancer. 1980;26:171–176.
28. Miyoshi T, Nagai T, Kikuchi S, et al. Cloning and characterization of a human BCR/ABL-positive cell line, K562/RR, resistant to the farne syltransferase inhibition by tipifarnib. Exp Hematol. 2007;35:1358–1365.
29. Lassar AB, Davis RL, Wright WE, et al. Functional activity of myogenic HLH proteins requires hetero-oligomerization with E12/E47-like proteins in vivo. Cell. 1991;66:305–315.
30. Uchida S, Yoshioka K, Kizu R, et al. Stress-activated mitogen-activated protein kinases c-Jun NH2-terminal kinase and p38 target Cdc25B for degradation. Cancer Res. 2009;69:6438–6444.
31. Zhu N, Shao Y, Xu L, Yu L, Sun L. Gadd45-alpha and Gadd45-gamma utilize p38 and JNK signaling pathways to induce cell cycle G2/M arrest in Hep-G2 hepatoma cells. Mol Biol Rep. 2009;36:2075–2085.
32. Moon DO, Kim MO, Choi YH, et al. Butein induces G(2)/M phase arrest and apoptosis in human hepatoma cancer cells through ROS generation. Cancer Lett. 2010;288:204–213.
33. Yoshida K, Nagai T, Ohmine K, et al. Vincristine potentiates the antiproliferative effect of an aurora kinase inhibitor, VE-465, in myeloid leukemia cells. Biochem Pharmacol. 2011;82:1884–1890.

34. Cluzeau T, Robert G, Puissant A, et al. Azacitidine-resistant SKM1 myeloid cells are defective for azacitidine-induced mitochondrial apoptosis and autophagy. Cell Cycle. 2011;10:2339–2343.
35. Marcucci G, Silverman L, Eller M, Lintz L, Beach CL. Bioavailability of azacitidine subcutaneous versus intravenous in patients with the myelodysplastic syndromes. J. Clin. Pharmacol. 2005;45:597–602.
36. Murata D, Endo Y, Obata T, et al. A crucial role of uridine/cytidine kinase 2 in antitumor activity of 3'-ethynyl nucleosides. Drug Metab Dispos. 2004;32:1178–1182.
37. Flasshove M, Strumberg D, Ayscue L, et al. Structural analysis of the deoxycytidine kinase gene in patients with acute myeloid leukemia and resistance to cytosine arabinoside. Leukemia. 1994;8:780–785.

**Supplementary Table 1.** Primers used for cDNA amplifications

| Genes | Forward | Reverse | Position |
|---|---|---|---|
| DNMT3a | 5′-acgacagcgatgagagtgac-3′ | 5′-cccaatcaccagatcgaatg-3′ | |
| DNMT3b-1 | 5′-aggaaagcatgaagggagacac-3′ | 5′-cagctggtcctccaatgagtct-3′ | 314–1,308 |
| DNMT3b-2 | 5′-atttggccaccttcaataagctc-3′ | 5′-ttcctcacgtcgttcacgtattt-3′ | 1,184–2,150 |
| DNMT3b-3 | 5′-cgcttctgaagtgtgtgaggagt-3′ | 5′-gtagtgcacaggaaagccaaaga-3′ | 2,067–2,706 |
| DNMT1-1 | 5′-gagatgccggcgcgtaccgc-3′ | 5′-gtgggtgctgcccatatttga-3′ | 178–1,342 |
| DNMT1-2 | 5′-ccaacggagaaaaaaatggct-3′ | 5′-tcccctggtgcatttttttgg-3′ | 1,231–2,401 |
| DNMT1-3 | 5′-agcaagcaggcttgccaagag-3′ | 5′-cgcactcgggcaggtcctccc-3′ | 2,281–3,451 |
| DNMT1-4 | 5′-ccagcgagctaccacgcagac-3′ | 5′-ccaccaatgcactcatgtcct-3′ | 3,331–4,501 |
| DNMT1-5 | 5′-tcggcactggagatctcctac-3′ | 5′-ttttggtttataggagagatttatttg-3′ | 4,372–5,403 |
| UCK2 | 5′-gcgaaccatggccggggacagcgag-3′ | 5′-acagtatgtacagatgagcagtgcc-3′ | |

**Supplementary Table 2.** Primers used for sequence analysis

| Genes | Forward | Reverse | Position |
|---|---|---|---|
| DNMT3a | 5′-gctttctggagtgtgcgtac-3′ | 5′-cccaatcaccagatcgaatg-3′ | |
| DNMT3b-1 | 5′-aggaaagcatgaagggagacac-3′ | 5′-agctcgcaccctagctttct-3′ | 314–1,308 |
| DNMT3b-2 | 5′-atttggccaccttcaataagctc-3′ | 5′-ggttccaacagcaatggact-3′ | 1,184–2,150 |
| DNMT3b-3 | 5′-cgcttctgaagtgtgtgaggagt-3′ | 5′-gagctcagtgcaccacaaaa-3′ | 2,067–2,706 |
| DNMT1-1 | 5′-gagatgccggcgcgtaccgc-3′ | 5′-agggtcgtccaggtactgc-3′ | 178–1,342 |
| DNMT1-2 | 5′-ccaacggagaaaaaaatggct-3′ | 5′-cggcatctctgggatgttat-3′ | 1,231–2,401 |
| DNMT1-3 | 5′-agcaagcaggcttgccaagag-3′ | 5′-acagccttgaagtccaccac-3′ | 2,281–3,451 |
| DNMT1-4 | 5′-ccagcgagctaccacgcagac-3′ | 5′-agatgtggtccctgaggatg-3′ | 3,331–4,501 |
| DNMT1-5 | 5′-tcggcactggagatctcctac-3′ | 5′-tttccactcatacagtggtagatttg-3′ | 4,372–5,403 |
| UCK2 | 5′-cgagcagaccctgcagaac-3′ | 5′-ccaagagacagaggaggggt-3′ | |

**Supplementary Table 3.** Primers used for real-time PCR

| Genes | Forward | Reverse |
|---|---|---|
| hENT1 | 5′-tctccaactctcagcccaccaa-3′ | 5′-cctgcgatgctggacttgacct-3′ |
| hENT2 | 5′-accatgccctccacctacag-3′ | 5′-gggcctgggatgatttattg-3′ |
| hCNT1 | 5′-acctcatagaagcagccagc-3′ | 5′-ccatcaagaaggagggctacaggc-3′ |
| P16 | 5′-agccttcggctgactggctgg-3′ | 5′-ctgcccatcatcatgacctgga-3′ |

# Interplay between CXCR2 and BLT1 Facilitates Neutrophil Infiltration and Resultant Keratinocyte Activation in a Murine Model of Imiquimod-Induced Psoriasis

Hayakazu Sumida,*,† Keisuke Yanagida,*,‡ Yoshihiro Kita,*,§ Jun Abe,¶ Kouji Matsushima,¶ Motonao Nakamura,* Satoshi Ishii,* Shinichi Sato,† and Takao Shimizu*,‡,§

**Psoriasis is an inflammatory skin disease with accelerated epidermal cell turnover. Neutrophil accumulation in the skin is one of the histological characteristics of psoriasis. However, the precise mechanism and role of neutrophil infiltration remain largely unknown. In this article, we show that orchestrated action of CXCR2 and leukotriene $B_4$ receptor BLT1 plays a key role in neutrophil recruitment during the development of imiquimod (IMQ)-induced psoriatic skin lesions in mice. Depletion of neutrophils with anti–Ly-6G Ab ameliorated the disease severity, along with reduced expression of proinflammatory cytokine IL-1β in the skin. Furthermore, CXCR2 and BLT1 coordinately promote neutrophil infiltration into the skin during the early phase of IMQ-induced inflammation. In vitro, CXCR2 ligands augment leukotriene $B_4$ production by murine neutrophils, which, in turn, amplifies chemokine-mediated neutrophil chemotaxis via BLT1 in autocrine and/or paracrine manners. In agreement with the increased IL-19 expression in IMQ-treated mouse skin, IL-1β markedly upregulated expression of acanthosis-inducing cytokine IL-19 in human keratinocytes. We propose that coordination of chemokines, lipids, and cytokines with multiple positive feedback loops might drive the pathogenesis of psoriasis and, possibly, other inflammatory diseases as well. Interference to this positive feedback or its downstream effectors could be targets of novel anti-inflammatory treatment.** *The Journal of Immunology*, **2014, 192: 4361–4369.**

Psoriasis is a persistent inflammatory skin disease thought to arise as a result of infiltration of inflammatory cells and activation of keratinocytes. Psoriasis has been considered as a classical type 1 autoimmune disease; recently, however, Th17 cells are attracting much interest. Biological drugs targeting the IL-23/IL-17 pathway achieved successful outcomes in psoriasis patients (1). Moreover, a massive amount of neutrophils and activated T cells infiltrates into psoriatic plaques (1). A role for IL-17 in neutrophil-mediated inflammation (2) suggests that neutrophils may also participate in the pathogenesis of psoriasis.

Neutrophils have been traditionally considered as an effector arm of innate immunity. However, recent studies suggest an intimate association of neutrophils with acquired immunity (3), suggesting a crucial role of neutrophils in the pathogenesis of a wide variety of diseases, including infections, autoimmunity, chronic inflammation, and cancer (4). In fact, various neutrophil chemoattractants are known to have unique functions in a number of human diseases (5). In psoriasis, neutrophils first infiltrate into the dermis at the early phase and later into the epidermis at the chronic phase (6). Moreover, neutrophil chemoattractants, including CXCL1, CXCL8 (also known as IL-8), and leukotriene $B_4$ ($LTB_4$), are upregulated in psoriatic skin (7, 8). A case report documented psoriasis remission during drug-induced agranulocytosis and its reappearance after the recovery of neutrophil numbers in the blood (9), suggesting a critical role of neutrophils in psoriatic skin inflammation. However, the detailed kinetics of neutrophil infiltration and its pathological role in psoriasis are still unknown.

Knowledge on the pathology of psoriasis has been obtained mostly through the study of human samples. However, the lack of appropriate animal models hindered addressing the mechanisms for the cellular and molecular events associated with the development of psoriatic lesion. Recently, topical application of imiquimod (IMQ) on the mouse skin has been reported to induce psoriasis-like inflammation (10). In this model, IMQ is suggested to exert its effects through adenosine receptor, but not TLR7 or TLR8, on keratinocytes, leading to the induction of proinflammatory cytokines (11). Importantly, IMQ model recapitulates the hallmarks of human psoriasis, including hyperkeratosis, erythema, scaling, neutrophil microabscesses in epidermis, and infiltration of γδ T cells and Th17 cells (10).

In this study, we investigated the significance of neutrophils in psoriasis using this IMQ-induced psoriasis model. Our data demonstrate that CXCR2 and BLT1 (also known as $LTB_4$ receptor 1 [Ltb4r1]) cooperatively act to promote neutrophil recruitment into psoriatic inflamed skin. Furthermore, we present evidence that the recruited neutrophils participate in the induction of psoriatic inflammation through IL-1β production.

*Department of Biochemistry and Molecular Biology, Faculty of Medicine, The University of Tokyo, Bunkyo-ku, Tokyo 113-0033, Japan; †Department of Dermatology, Faculty of Medicine, The University of Tokyo, Tokyo 113-8655, Japan; ‡Department of Lipid Signaling, National Center for Global Health and Medicine, Tokyo 166-8655, Japan; §Department of Lipidomics, Faculty of Medicine, The University of Tokyo, Tokyo 113-0033, Japan; and ¶Department of Molecular Preventive Medicine, Graduate School of Medicine, The University of Tokyo, Tokyo 113-0033, Japan

Received for publication November 1, 2013. Accepted for publication February 21, 2014.

This work was supported by grants-in-aid for scientific research from the Ministry of Education, Culture, Sports, Science and Technology of Japan (M.N., S.I., T.S.) and the Global Center of Excellence Program of The University of Tokyo from the Japan Society for Promotion of Sciences (T.S.).

Address correspondence and reprint requests to Dr. Hayakazu Sumida, Department of Biochemistry and Molecular Biology, Faculty of Medicine, The University of Tokyo, 7-3-1 Hongo, Bunkyo-ku, Tokyo 113-0033, Japan. E-mail address: sumida-tky@umin.ac.jp

The online version of this article contains supplemental material.

Abbreviations used in this article: Alox5, arachidonate 5-lipoxygenase; IHS, immunohistochemical staining; IMQ, imiquimod; KO, knockout; 5-LOX, 5-lipoxygenase; $LTB_4$, leukotriene $B_4$; qPCR, quantitative real-time PCR; WT, wild-type.



www.jimmunol.org/cgi/doi/10.4049/jimmunol.1302959

## Materials and Methods

### *Mice*

*Ltb4r1*-knockout (KO) mice were described previously (12). *Ccr2*-KO mice were purchased from The Jackson Laboratory. All mice used in this study were on a C57BL/6 background and kept under specific pathogen-free conditions with food and water ad libitum. All experiments were approved by the Institutional Animal Care and Use Committee of The University of Tokyo.

### *IMQ-induced psoriasis model*

Mice at 8–12 wk of age received a daily topical dose of 30 mg 5% IMQ cream (Beselna Cream; Mochida Pharmaceutical, Tokyo, Japan) on shaved backs for 6 consecutive days. Based on a previously described objective scoring system called Psoriasis Area and Severity Index (10), erythema, scaling, and thickness were scored independently on a score from 0 to 4: 0, none; 1, slight; 2, moderate; 3, marked; 4, very marked. The cumulative score (erythema plus scaling plus thickness) served as the measure of the severity (score 0–12).

### *Quantitative real-time PCR*

After sacrificing the mice, 6-mm punch biopsies were obtained from the back skin, and total RNA was isolated using the RNeasy Fibrous Tissue Mini Kit (QIAGEN). Using 1 μg total RNA template, we prepared cDNA using SuperScript III reverse transcriptase and random primers (Invitrogen Life Technologies). mRNA levels were measured by quantitative real-time PCR (qPCR) analysis using the LightCycler System (Roche; for primers, see Supplemental Table I). The PCRs were set up in microcapillary tubes in a volume of 20 μl, consisting of 2 μl cDNA solution, 1 × FastStart DNA Master SYBR Green I, and 0.5 μM each sense and antisense primers. The PCR program was as follows: denaturation at 95°C for 3 min and 45 cycles of amplification consisting of denaturation at 95°C for 15 s, annealing at 65°C for 5 s, and extension at 72°C for 7 s. Data were normalized to *Rplp0* (also known as *36B4*) expression levels.

### *Measurement of cytokine and chemokine levels in IMQ-treated skin*

Cytokine and chemokine concentrations in the total skin were measured by ELISA as described previously with minor modifications (13). In brief, three samples of 3-mm full-thickness punch biopsies were obtained from IMQ-treated mouse back skin and were incubated in 450 μl PBS with Complete protease inhibitors (Roche). The biopsy fragments were shaken in the solution at 4°C for 3 h. The supernatant was collected after centrifugation at 12,000 × *g* for 5 min at 4°C, and protein concentrations were measured with commercially available ELISA kits (R&D Systems).

### *Immunohistochemical staining of skin sections for Gr-1*

Dorsal skin samples were obtained from 6-mm punch biopsies, embedded in OCT compound (Tissue-Tek, FL; Sakura Finetek, Tokyo), and snap-frozen in liquid nitrogen. Immunohistochemical staining (IHS) was performed using the Vectastain ABC peroxidase kit (Vector Laboratories). In brief, sections were blocked with diluted normal blocking serum and were incubated with primary rat anti-mouse Gr-1 (clone RB6-8C5) mAb (eBioscience) diluted at 1:200. Sections were further incubated with biotinylated donkey anti-rat IgG secondary Ab (Jackson Immunoresearch Laboratories). Immunoreactivity was detected by incubating with the 3,3′-diaminobenzidine peroxidase substrate kit (Vector Laboratories). Sections were then counterstained with hematoxylin.

### *In vivo administration of anti–Ly-6G mAb to deplete neutrophils*

As reported previously (14), wild-type (WT) mice were i.p. injected every other day from days −2 to 4 with 500 μg rat anti-mouse Ly-6G Ab (clone 1A8; BioXCell) or rat IgG2a (clone 2A3; BioXCell) dissolved in 200 μl PBS. Skin samples on day 2 and 4 were fixed in 10% formalin for H&E staining or embedded in OCT compound and frozen for immunohistochemical analysis. IHS of day 2 skin samples revealed successful depletion of Gr-1$^+$ cells by anti–Ly-6G mAb treatment (Fig. 1D).

### *In vivo administration of SB225002*

Mice received daily i.p. injection of 1 mg/kg selective CXCR2 antagonist SB225002 (Cayman Chemical) or vehicle from days −1 to 5. SB225002 was dissolved in saline containing 0.33% Tween 80 just before use.

### *Cell culture*

HaCaT cells were routinely cultured in DMEM (Nacalai Tesque) supplemented with 10% FBS. In some experiments, cells were serum starved for indicated times. For the stimulation, cells were treated with IMQ (5 μg/ml; Invivogen), IL-1β (10 ng/ml; Wako), or vehicle for the indicated times. Total RNA was prepared from the treated cells by using the RNeasy Mini kit (Qiagen).

### *Neutrophil isolation from the IMQ-treated skin*

For neutrophil isolation from the skin tissue, harvested skin samples were cut in pieces with scissors and digested with 0.14 U/ml Liberase DH (Roche) and 100 μg/ml DNase I (Roche) in RPMI 1640 medium (Sigma) for 1.5 h. Single-cell suspension was prepared by passing the digested tissues through a 70-μm cell strainer (BD) and shredding with gentleMACS Dissociator (Miltenyi Biotec). Gr-1$^+$ cells were enriched by positive selection using autoMACS (Miltenyi Biotec). Successful separation was confirmed by flow cytometry.

### *RT-PCR analysis*

Total RNA was purified from MACS-sorted Gr-1$^-$ and Gr-1$^+$ cells obtained from IMQ-treated skin tissue as described earlier. cDNA was synthesized using SuperScript III reverse transcriptase and random primers. The resultant cDNA was amplified by PCR. The protocol and sequences of primers used to measure *Ltb4r1*, *arachidonate 5-lipoxygenase* (*Alox5*), and *Actb* (also known as *β-actin*) levels were described previously (15).

### *Quantification of $LTB_4$ levels in skin tissue*

$LTB_4$ levels were measured as described previously (16). In brief, dorsal skin samples were obtained from 6-mm punch biopsies, frozen immediately in liquid nitrogen, and stored at −80°C until use. The frozen tissues (50–100 mg) were powdered with Auto-Mill (Tokken, Chiba City, Japan), and lipids were extracted for 1 h at 4°C with methanol. $LTB_4$ levels were quantified by reversed phase HPLC electrospray ionization-tandem mass spectrometry methods.

### *In vivo administration of zileuton and CP105696*

Mice were given daily oral administration of 50 mg/kg 5-lipoxygenase (5-LOX) inhibitor zileuton (Sigma), 10 mg/kg BLT1 antagonist CP105696 (a kind gift from Pfizer), or vehicle (0.5% methylcellulose), starting 1 d before the first IMQ treatment.

### *Isolation of peritoneal neutrophils*

Neutrophils were obtained from the peritoneal exudates 3–4 h after i.p. injection of 3% thioglycolate at a dose of 2 ml/25 g (BD). For cell cultures, Gr-1$^+$ cells were isolated from peritoneal exudates by using an autoMACS cell separator. Purity of the isolated Gr-1$^+$ cells was >95%. Purified cells were subjected to chemotaxis assay or RNA extraction using the RNeasy Mini Kit (Qiagen).

### *Chemotaxis assays*

Chemotaxis assays were performed by using HTS Transwell 96-well plates with 3-μm pores (Corning). Mouse peritoneal neutrophils were resuspended in RPMI 1640 medium supplemented with 0.25% BSA (fatty acid free; Sigma). The cells were added into the upper wells (5 × $10^4$ cells/well), and 100 ng/ml CXCL2 (Biolegend), 100 ng/ml CXCL1 (Biolegend), or 10 nM $LTB_4$ (Cayman) was added to the lower wells. In some experiments, resuspended neutrophils were pretreated with vehicle, zileuton (50 μM), or CP105696 (1 μM) for 30 min. The plates were incubated at 37°C for 3 h. After removing the upper wells, we determined the number of migrated cells by using the CellTiter-Glo Luminescent Cell Viability Assay (Promega). Data were normalized with the results from vehicle-treated samples and expressed as relative light unit.

### *Quantification of released $LTB_4$ from peritoneal neutrophils stimulated by CXCR2 ligands*

The effect of CXCL2 or CXCL1 on $LTB_4$ production was studied using peritoneal neutrophils (1 × $10^6$ cells suspended in 200 μl HBSS), challenged either with CXCL2 (100 ng/ml, 10 min, 37°C) or CXCL1 (100 ng/ml, 10 min, 37°C) after preactivation with GM-CSF (50 ng/ml, 30 min, 37°C). Incubations were terminated by rapid pelleting of cells at 4°C. Supernatants were collected and frozen immediately at −80°C. $LTB_4$ levels in supernatant samples were determined by ELISA kits (Cayman Chemical) following the manufacturer's instructions.

*Statistical analysis*

Data were expressed as the mean ± SEM and analyzed using GraphPad Prism 4 software (GraphPad Software). Statistical significance was determined by either two-tailed Student *t* test, one-way ANOVA followed by Dunnett's post hoc test, or two-way ANOVA followed by Bonferroni's post hoc test as indicated in the figure legends. A $p$ value $<0.05$ was considered statistically significant.

## Results

*Infiltration of Gr-1$^+$ cells and elevated IL-1β level in IMQ-treated skin during the development of psoriatic lesions*

To characterize the IMQ-induced skin inflammation, we first investigated the kinetics of expression of *Krt16* as an epithelial differentiation marker, *Il23a* (also known as *IL-23 p19*) as a cytokine driving the development of Th17 cells, and *IL17a* as a Th17 cytokine. In agreement with published studies (10), these markers were induced with a peak on day 3 (Fig. 1A). The mRNA level of TNF-α, another key proinflammatory cytokine in psoriasis, was also found to be increased transiently on day 2 (Supplemental Fig. 1). Associated with these findings, mRNA encoding neutrophil marker Ly-6G was found to show a transient increase that peaked on day 2 (Fig. 1A). Accordingly, we also observed the infiltration of Gr-1 (also known as Ly-6G/C)-positive cells in IMQ-treated skin on day 2 (Fig. 1B). Furthermore, polymorphonuclear leukocytes infiltrated into IMQ-treated skin were observed on day 2 by H&E staining (Fig. 1C). In support of these findings, the kinetics of mRNA expression and protein level of a neutrophil-derived cytokine IL-1β were congruent with the expression of Ly-6G (Fig. 1A, 1D). Macrophages are also known to produce IL-1β, as well as neutrophils. In contrast with the kinetics of *Ly6g* and *Il1b* expression, however, the kinetics of EGF-like module-containing, mucin-like, hormone receptor-like sequence 1 (Emr1, also known as F4/80) mRNA showed only a marginal increase on day 1 (Supplemental Fig. 1). These findings raise the possibility that neutrophils might be the main source of secreted IL-1β. Because IL-1β is implicated in the pathogenesis of psoriasis (17), neutrophils likely play important roles in psoriatic skin inflammation as the primary cellular source of IL-1β.

*Contribution of neutrophils, but not macrophages, to IMQ-induced psoriatic skin inflammation*

Next, we attempted to demonstrate the role of neutrophils in IMQ-induced skin inflammation by using neutrophil depletion with anti–Ly-6G (clone 1A8) Ab (18) in the IMQ model. IHS confirmed the successful depletion of neutrophils by anti–Ly-6G Ab treatment (Fig. 2A). Assessment of disease severity by using Psoriasis Area and Severity Index score (10) revealed that neutrophil depletion alleviated the psoriatic symptoms compared with control IgG-treated mice (Fig. 2B, 2C). In addition, histological examination showed that inflammatory cellular infiltration, epidermal thickening, and dermal thickening in neutrophil-depleted mice were all attenuated (Fig. 2D). In stark contrast, mice deficient in the gene encoding CCR2 with defective monocyte egress from bone marrow (19) exhibited comparable scores with those of WT mice (Fig. 2E). These results indicate that neutrophils, but not macrophages, contribute to psoriatic skin inflammation in this model.

*Involvement of CXCR2 in neutrophil recruitment in IMQ-induced psoriatic skin*

Next, we sought to identify the chemoattractants responsible for initial neutrophil recruitment in the IMQ model. Because the mRNA of CXCR2, one of the representative molecules responsible for neutrophil recruitment, is upregulated in epidermis and detected in infiltrated dermal polymorphonuclear cells in human psoriatic skin (20), we first focused on the role of CXCR2 in this model. mRNA level of CXCR2 in IMQ-treated skin was increased with progression of psoriatic skin (Fig. 3A). Both mRNA and protein levels of CXCR2 ligands CXCL2 (also known as MIP-2) and CXCL1 (also known as keratinocyte-derived chemokine) were transiently elevated (Fig. 3A, 3B) in parallel with *Ly6g* and *Cxcr2* expression levels and neutrophil infiltration. Consistent with a previous study, IMQ induced the expression of CXCR2 ligands in human keratinocyte cell line HaCaT cells in vitro (Supplemental Fig. 2A), suggesting that keratinocytes stimulated with IMQ may initiate neutrophil recruitment in the IMQ model. These results prompted us to hypothesize that CXCR2 and its ligands might contribute to initial neutrophil recruitment in early phase of psoriasis. We tested

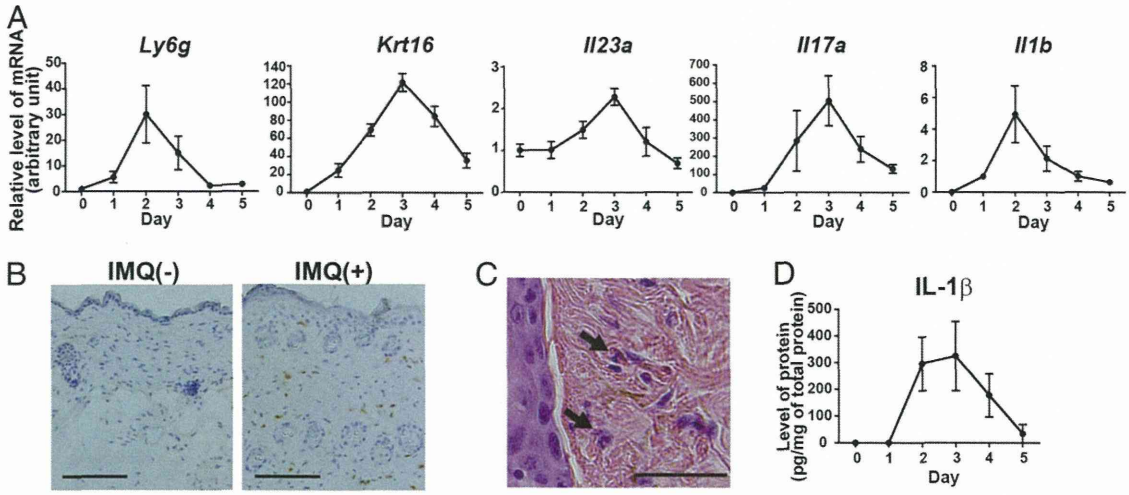


**FIGURE 1.** Infiltration of neutrophils in IMQ-induced psoriasis-like skin inflammation. (**A**) Kinetics of the mRNA levels of Ly-6G, IL-1β, Krt16, IL-23p19, and IL-17A in IMQ-treated skin tissue from individual WT mice ($n = 5$ mice for each time point [days 0, 1, 2, 3, 4, and 5]). Representative data from one of two independent experiments are shown. (**B**) IHS analysis of neutrophil infiltration in nontreated (*left panel*, IMQ$^-$) or IMQ-treated (right panel, IMQ$^+$) skin on day 2. Images are representative of five mice from three independent experiments in each group. Scale bars, 100 μm. (**C**) H&E staining of IMQ-treated skin from WT mice on day 2. A representative of five mice from three independent experiments is shown. Black arrows highlight individual polymorphonuclear neutrophils. Scale bar, 50 μm. (**D**) Released IL-1β protein levels in IMQ-treated skin from WT mice ($n = 4$–7 mice for each time point). Representative data from two independent experiments.

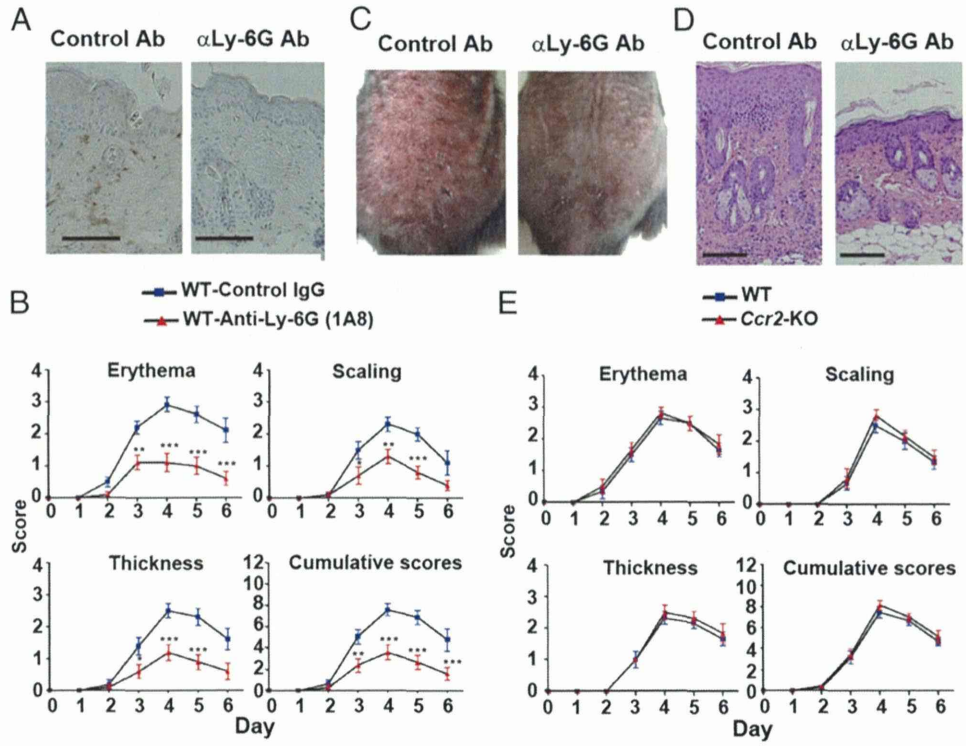


**FIGURE 2.** Attenuated psoriatic skin inflammation by neutrophil depletion. (**A**) IHS analysis of neutrophil infiltration on day 2 in IMQ-treated skin from mice administered rat IgG2a (*left*) or anti–Ly-6G mAb (*right*). Images are representative of four mice from two independent experiments in each group. (**B**) Time course of the scores in mice administered rat IgG2a or anti–Ly-6G mAb ($n = 6$ mice for each group in each time point). Two-way ANOVA followed by Bonferroni's post hoc test. (**C**) IMQ-treated back skin of mice administered rat IgG2a (*left panel*) or anti–Ly-6G mAb (*right panel*) on day 4. Images are representative of six mice from three independent experiments in each group. (**D**) H&E staining of IMQ-treated skin from mice administered rat IgG2a (*left panel*) or anti–Ly-6G mAb (*right panel*) on day 4. Images are representative of five mice from two independent experiments in each group. (**E**) Time course of scores in WT or *Ccr2*-KO mice ($n = 6$ mice for each group in each time point). Representative data from one of two (E) or three (B) independent experiments are shown. Scale bars, 100 μm (A and D). $*p < 0.05$, $**p < 0.01$, $***p < 0.001$.

this by using a selective CXCR2 antagonist, SB225002. As expected, Gr-1$^+$ neutrophil infiltration was reduced by SB225002 administration (Fig. 3C), demonstrating an important role of CXCR2 in neutrophil recruitment in IMQ-induced dermatitis. Of note, SB225002 treatment also attenuated symptoms (Fig. 3D), which is consistent with the effect of neutrophil depletion by anti–Ly-6G Ab (Fig. 2B).

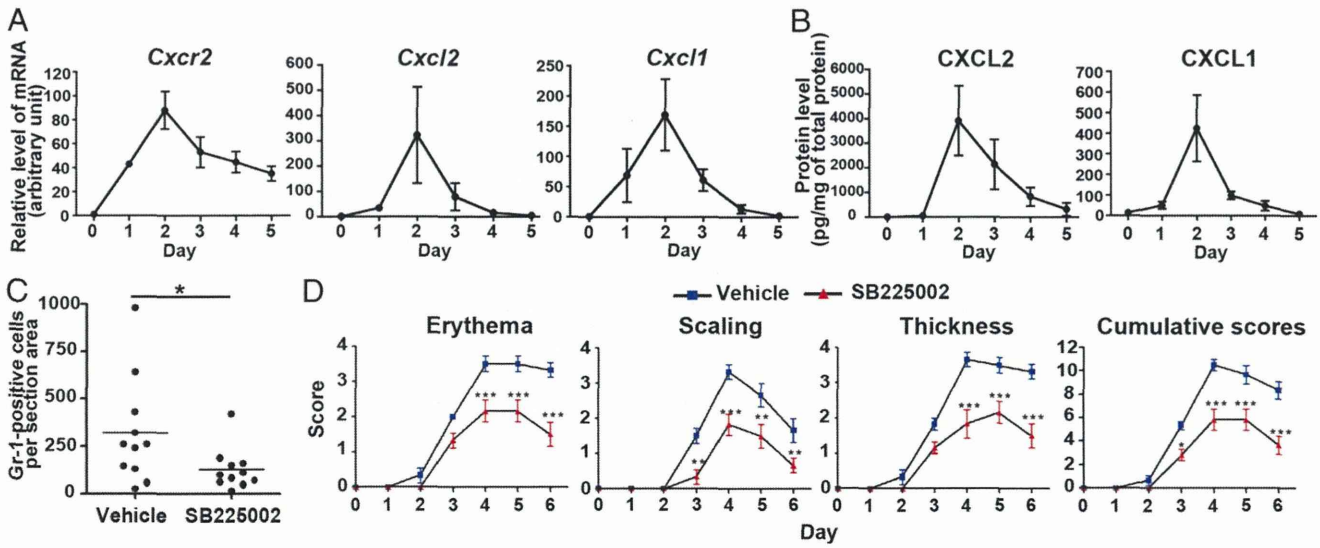


**FIGURE 3.** Role of CXCR2 in IMQ-induced psoriasis-like skin inflammation. (**A**) mRNA of neutrophil-related chemokines and their receptors in IMQ-treated skin tissue from individual WT mice ($n = 5$ mice for each time point). (**B**) CXCL2 and CXCL1 protein levels in IMQ-treated skin from individual WT mice ($n = 4$–7 mice for each time point). (**C**) Number of Gr-1$^+$ cells in IMQ-treated back skin of WT mice administered vehicle or SB225002 ($n = 11$ mice for each group). (**D**) Time course of scores in WT mice administered vehicle or SB225002 ($n = 7$ mice for each group in each time point). Representative data from one of two independent experiments are shown. Two-tailed Student *t* test (C). Two-way ANOVA followed by Bonferroni's post hoc test (D). $*p < 0.05$, $**p < 0.01$, $***p < 0.001$.

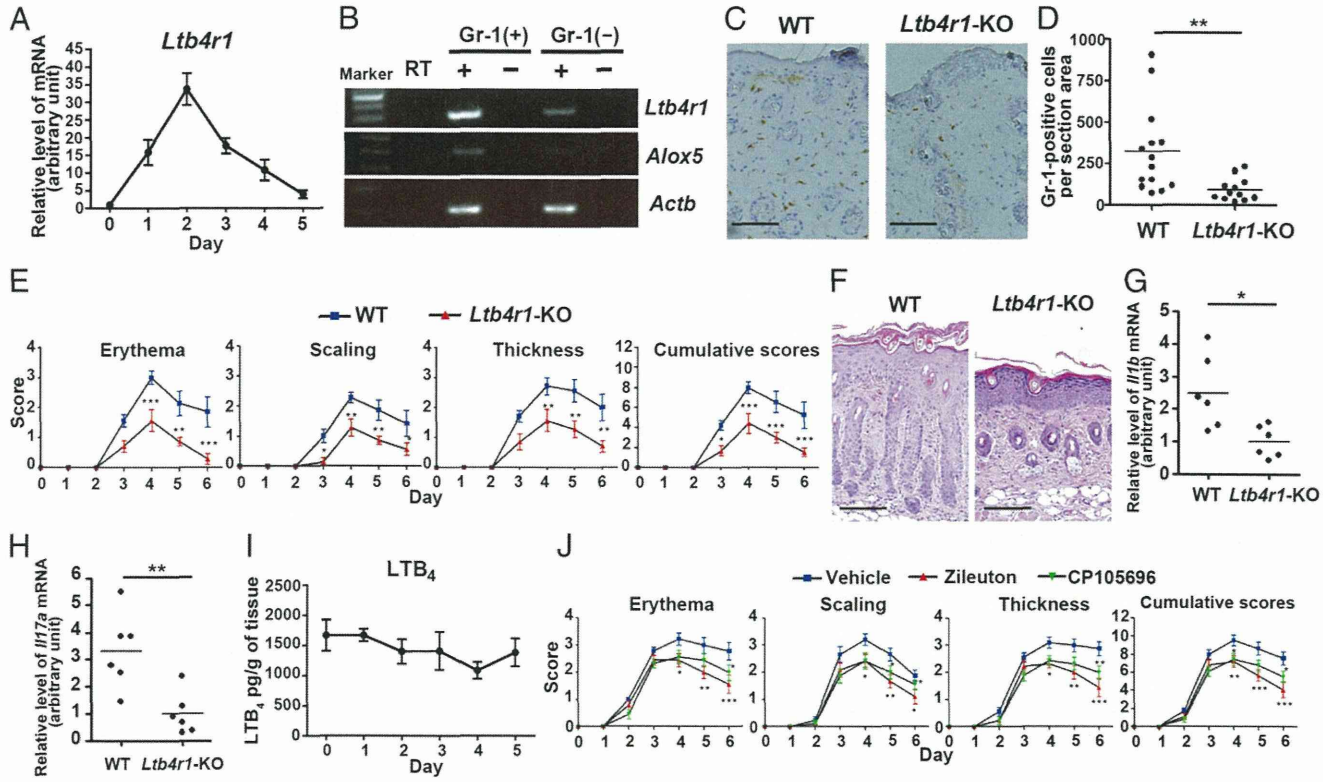


**FIGURE 4.** Role of BLT1 in IMQ-induced psoriasis-like skin inflammation. (**A**) *Ltb4r1* expression in IMQ-treated skin tissue. (**B**) BLT1 and 5-LOX mRNA expression in Gr-1$^+$ and Gr-1$^-$ cells obtained from IMQ-treated skin. (**C**) IHS analysis of neutrophil infiltration on day 2 in WT (*left panel*) or *Ltb4r1*-KO (*right panel*) mice. (**D**) Numbers of Gr-1$^+$ cells per cross-sectional area of 6-mm punch in IMQ-treated back skin from mice ($n$ = 14 or 12 mice for WT or *Ltb4r1*-KO, respectively). (**E**) Time course of the scores in WT or *Ltb4r1*-KO mice ($n$ = 7 mice for each group in each time point). (**F**) H&E staining of the skin from WT (*left panel*) or *Ltb4r1*-KO (*right panel*) mice on day 4. (**G** and **H**) Expression of IL-1β (G) and IL-17A (H) mRNA in WT and *Ltb4r1*-KO skin on day 2. Each dot represents one mouse ($n$ = 6 mice for each group). (**I**) $LTB_4$ level in IMQ-treated skin tissue from mice ($n$ = 5 mice for each group). (**J**) Time course of the scores in mice administered vehicle, zileuton, or CP105696 ($n$ = 9 mice for each group in each time point). Representative data from one of two (A, B, D, and G–J) or three (E) independent experiments are shown. Two-tailed Student $t$ test (D, G, and H). Two-way ANOVA followed by Bonferroni's post hoc test (E and J). $*p < 0.05$, $**p < 0.01$, $***p < 0.001$. Scale bars, 100 μm. RT, reverse transcription; RT(+), reverse transcribed; RT(−), no reverse transcription.

*Involvement of BLT1 in neutrophil recruitment in IMQ-induced psoriatic skin*

Although SB225002 alleviated psoriatic skin inflammation, it was not as efficient as neutrophil depletion. We surmised that this was due to the presence of additional chemoattractants involved in this process. $LTB_4$, the ligand for the G protein–coupled receptor BLT1 (21), is a potent chemoattractant for neutrophils (22) and could serve as such a candidate. Expression of BLT1 mRNA transiently increased on day 2 (Fig. 4A), as observed for Ly-6G mRNA expression and neutrophil infiltration. The source of this BLT1 mRNA was found to be Gr-1$^+$ neutrophils (Fig. 4B) by RT-PCR analysis with isolated Gr-1$^+$ cells from IMQ-treated skin. The results suggest a role for BLT1 in the recruitment of neutrophils to psoriatic skin. In fact, *Ltb4r1*-KO mice exhibited markedly attenuated neutrophil infiltration (Fig. 4C, 4D) and reduced mRNA expression of Ly-6G (Supplemental Fig. 3A). Disease severity in *Ltb4r1*-KO mice was also decreased compared with WT mice (Fig. 4E, 4F, Supplemental Fig. 3B). In addition, we also found reduced *Il1b* expression in the skin of *Ltb4r1*-KO mice (Fig. 4G). Furthermore, *Ltb4r1*-KO mice showed reduced mRNA expression of IL-17A (Fig. 4H), which is considered to play a pivotal role in the pathogenesis of psoriasis (1). These results suggest that reduced IL-1β level caused by attenuated neutrophil infiltration may account for the difference in psoriatic phenotypes observed between WT and *Ltb4r1*-KO. To support this idea, WT mice given anti–Ly-6G Ab and *Ltb4r1*-KO mice given control IgG showed the same degree of scores (Supplemental Fig. 3C), indicating the possibility that the reduction of scores in *Ltb4r1*-KO might be largely caused by attenuated neutrophil infiltration. In addition, in IMQ-treated mice given anti-Ly6G Ab, BLT1 deficiency slightly tended to reduce scores compared with WT (Supplemental Fig. 3C), suggesting the contribution of other unknown factors except for neutrophils.

*IMQ-induced psoriatic skin requires 5-LOX pathway*

$LTB_4$ is a major product of arachidonic acid metabolism and is synthesized via the 5-LOX, also known as Alox5, pathway (23, 24). By activating $LTB_4$ receptors, $LTB_4$ exerts its biological effects in host immune response and in pathogenesis of various inflammatory diseases (25). In contrast with the increase in BLT1 mRNA levels, $LTB_4$ levels remained constant in IMQ-treated mouse skin from days 0 to 6 (Fig. 4I). Despite the absence of upregulation of $LTB_4$, mice treated with a 5-LOX inhibitor zileuton showed disease symptoms as mild as those treated with a BLT1 antagonist CP105696 (Fig. 4J). These results and the expression of *Alox5* in Gr-1$^+$ neutrophils (Fig. 4B) suggest that $LTB_4$ production in the proximity of neutrophils may be involved in the exacerbation of psoriatic inflammation. Another possibility is that basal $LTB_4$ level in mouse skin is sufficient for the induction of psoriatic dermatitis.

*Amplification of CXCR2 ligand–induced neutrophil chemotaxis by $LTB_4$–BLT1 axis in vitro*

The concurrent expression of *Cxcr2* and *Ltb4r1* prompted us to hypothesize that these factors cooperatively regulate neutrophil infiltration. To test this hypothesis, we performed in vitro chemotaxis